REFINING POROSITY ANALYSIS IN HIGH-STRENGTH MICROCONCRETES THROUGH MANUAL THRESHOLD SEGMENTATION IN X-RAY MICROTOMOGRAPHY

Arthur Aviz Palma e Silva[1*] Valdirene Maria Silva Capuzzo[2] Eugênia Fonseca da Silva[3] André Maués Brabo Pereira[4]

[1] PhD candidate in Structures and Civil Construction at the University of Brasília (UnB), Brasília - DF, Brazil;

[2] Department of Civil and Environmental Engineering, Professor of the Graduate Program in Structures and Civil Construction at the University of Brasília (UnB), Brasília - DF, Brazil;

[3] Department of Civil and Environmental Engineering, Researcher of the Graduate Program in Structures and Civil Construction at the University of Brasília (UnB), Brasília - DF, Brazil;

[4] Materials Digital Laboratory, Fluminense Federal University (UFF), Rio de Janeiro - RJ, Brazil.

Corresponding author: eng.aviz@gmail.com

ABSTRACT

The present study aimed to assess the effectiveness of the image segmentation technique utilizing the Threshold method for the measurement of porosity in high-strength microconcrete samples that incorporate metakaolin. Specifically, X-ray microtomography testing was conducted on the microconcrete samples after 7 days of curing, and the voxel size was set at 20µm. Subsequently, the images were subjected to pre-processing measures including histogram regularization and noise reduction. Thereafter, the regions of interest within the images were demarcated through segmentation, enabling the isolation of the porosity from the other phases of the microconcrete. To execute the segmentation, grayscale values were systematically adjusted via the Threshold method to elucidate the impact of such variations on the determination of porosity properties. The study findings indicate that the proposed technique yields reliable measurements of the total porosity percentage of the material, despite the human factor inherent in the manual Threshold segmentation approach. However, caution should be exercised while performing segmentation when assessing pore quantity and dimensions as these are substantially influenced by this technique.

KEYWORDS: *Microconcrete, Porosity Measurement, Image Segmentation, Threshold Method, X-Ray Microtomography, Metakaolin.*

I. INTRODUCTION

X-ray microtomography (Micro-CT) is a reliable and accurate technique for conducting thorough evaluations of materials at various scales. This advanced technology allows for the visualization of different types of defects, including fractures, cracks, minerals, grains, and voids, which are crucial for assessing the quality of a solid body [1]. Digital image analysis using Micro-CT involves multiple stages, such as computational model acquisition, sample preparation, data acquisition, microtomographic reconstruction, segmentation, model mesh generation, and computational simulations.

The Micro-CT technique generates 3D images of either the entire test specimen or a portion of it, depending on the requirements. Sample preparation is relatively straightforward, requiring the specimen to be of suitable size and shape to fit the equipment. Additionally, most of the time, the image acquisition process is non-destructive, allowing for a large amount of data to be obtained from a single

sample [2]. Fragmented samples can also be analyzed, which enables a more detailed visualization of an object's microstructure, but at the cost of its integrity due to the fragmentation. According to Bernardes et al. [3], it is essential to consider the sample size when using Micro-CT since smaller samples may not be representative of the entire object, which can be problematic.

After obtaining a 3D reconstruction of a material, it is possible to visualize it from various angles and even slice it in specific planes to analyze its microstructure. However, to examine properties related to voids such as porosity and permeability, specific processing methods are required. These methods involve the application of filters for noise reduction and image correction to segment regions of interest [4].

Rattanasak and Kendall [5] conducted a study using Micro-CT technique to investigate porosity and pore characteristics in cement mortars with pozzolanic compounds. They analyzed three samples, including one with 25% Portland cement substitution by fly ash, a second with 10% substitution by kaolinite, and a third reference sample without substitution. The results revealed that the kaolinite-substituted sample had smaller pore sizes compared to the fly ash-substituted sample. The reference mixture with Portland cement, without substitution, had the largest average pore size.

Palma e Silva et al. [6] employed X-ray microtomography to quantify pores in high-strength microconcrete cementitious mixtures containing metakaolin and superabsorbent polymer. They concluded that the polymer could increase the mixture's porosity. The authors used the Threshold segmentation method, which involves manually separating the region of interest from the material by inputting specific data to segment a particular area. Meira et al. [7] have discussed the effectiveness of the manual segmentation method using a pre-defined threshold in their research work. They analyzed five different threshold bands and found that there was only a 0.45% variation between them. Enríquez-León et al. [8] conducted a study on Micro-CT image segmentation methods in asphalt to determine the porosity of the samples. Their research demonstrated that the values obtained using the threshold segmentation method were similar to those obtained by other techniques, such as Machine Learning and Deep Learning.

This article aimed to evaluate the current effectiveness of the Threshold segmentation method in high-strength microconcretes containing metakaolin, by extensively varying the segmentation parameters. Eleven segmentations were performed with different parameters to establish relationships between them.

Segmentation is a pivotal technique in image analysis, as it facilitates the separation of various components within an image. However, the appropriate selection of segmentation parameters is crucial to ensure accurate and dependable results. In this study, the impact of distinct segmentation parameters on the precision and quality of the obtained outcomes was analyzed, contributing to the development of more sophisticated and effective image analysis techniques in high-strength microconcretes containing metakaolin. The paper is divided into six sections. The first section provides an Introduction, while the second section outlines the Methodology, including the materials and procedures used. The third section presents the Results and Discussions, followed by the fourth section that offers a Conclusion. The fifth section comprises the Acknowledgments, while the sixth section provides the References.

II. METHODOLOGY

2.1. Materials

In this study, high initial strength Portland cement CPV-ARI, as specified in Table 1 of ABNT NBR 16697 [9], was used as the binder. Metakaolin was also added to the concrete mixtures to enhance its strength at later ages due to its pozzolanic effect, making it an effective product for concrete production in the Brazilian market. Table 2 presents the material properties of metakaolin. The mineralogical characterization of the metakaolin used in this study was carried out using the X-ray diffraction (XRD) technique and can be seen in Figure 1.

Table 1. Binder characterization.

Properties		Minimum requirements[(a)]	CP - V	Method
Initial setting time (min)		≥ 60	140	ABNT NBR 16607 [10]
Final setting time (min)		≤ 600	180	
Specific Gravity (Kg/ m³)		-	3.02	ABNT NBR 16605 [11]
Dimeter below which 10% of the particles are – D10 (µm)		-	1.30	X – Ray Diffraction
Dimeter below which 50% of the particles are – D50 (µm)			13.10	
Dimeter below which 90% of the particles are – D90 (µm)			31.76	
Compressive strength	1 day	≥ 14	21.54	ABNT NBR 7215 [12]
	3 days	≥ 24	39.37	
	7 days	≥ 34	44.42	
	28 days	-	52.26	
Oxide's composition (%)	*SiO_2*	-	15.03	X- Ray fluorescence spectroscopy
	CaO	-	72.25	
	Mgo		0.87	
	Al_2O_3	-	3.88	
	Fe_2O_3	-	3.01	
	K_2O	-	0.32	
	TiO_2	-	0.34	
	ZaO	-	0.01	
	SO_3	≤ 4.5%	3.7	
	MnO	≤ 6.5 %	0.06	
Loss on Ignition (%)		≤ 6.5 %	6.12	
[(a)]Limits by ABNT NBR 16697 [9]				

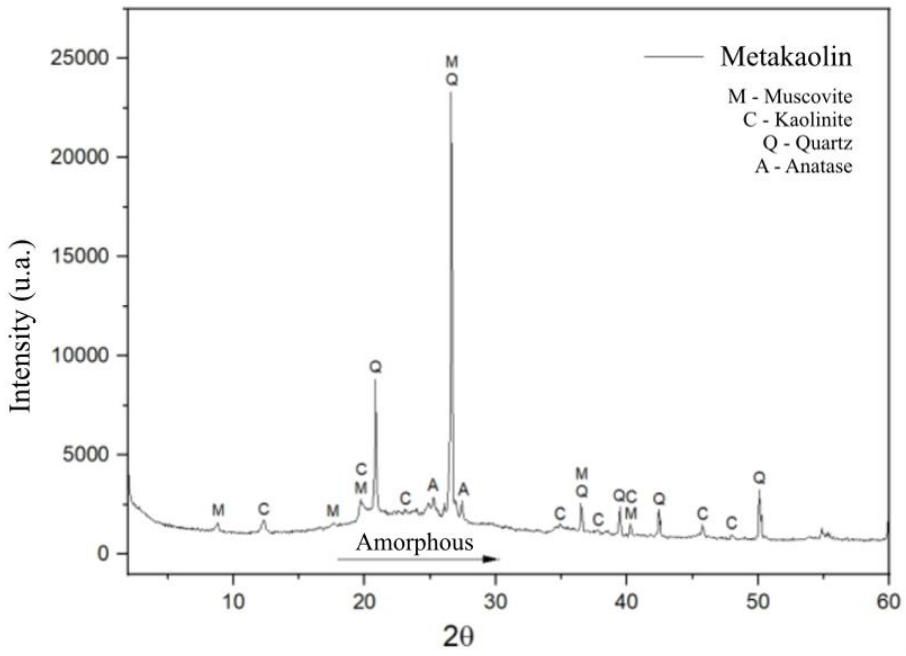

Figure 1. Metakaolin properties

Table 2: Metakaolin characterization.

Properties		Metakaolin	Method
Specific Gravity (g/ m³)		2.54	ABNT NBR 16605 [11]
Dimeter below which 10% of the particles are – D10 (µm)		1.47	X – Ray diffraction
Dimeter below which 50% of the particles are – D50 (µm)		14.16	
Dimeter below which 90% of the particles are – D90 (µm)		42.02	
Oxide's composition (%)	SiO_2	54.54	X- Ray fluorescence spectroscopy
	CaO	0	
	Mgo	0	
	Al_2O_3	38.73	
	Fe_2O_3	2.94	
	K_2O	1.77	
	TiO_2	1.7	
	ZaO	0.01	
	SO_3	0.07	
	MnO	0.01	
	SrO	0.01	
	$Se2O3$	0	
	Zno	0.01	
Loss on ignition (%)		2.59	

The research employed a natural, quartz-based fine aggregate that was meticulously selected from the Corumbá River located in the Brasília-DF region. Table 3 provides the results of physical characterization tests conducted on the sand used in this study, in accordance with the relevant normative recommendations.

Table 3: Fine aggregate properties

Fine aggregate	Results
Bulk density (g/m³)	2.63
Loose bulk density (g/cm³)	1.58
Fineness modulus	2.60
Maximum dimension (mm)	6.3
Water absorption (%)	1%

The specific mass and loose unit mass of a quartzose sand extracted from a river and washed were found to be within the expected range. This sand was utilized in its raw form, without any treatment or mixture with other materials. The delineated zones of the sand were identified according to the ABNT NBR 7211 [13] standard, which designates optimal and usable zones. The chosen sand falls within the optimal zone established by ABNT NBR 7211 [13] and the recommendations of the RILEM TC 255 - SAP [14] committee.

In order to attain the research objectives, a highly efficient water-reducing additive was necessary for high-strength micro-concrete mixes. These mixes had a low water-to-cement ratio of 0.35, making it challenging to mold specimens. The additive used was GLENIUM-51, a third-generation superplasticizer from BASF company, which is based on polycarboxylate and normal setting (N). This additive is characterized by a recommended dosage range of 0.2-1.0%, milky white color, density of 1.067-1.107 g/cm³, and a solid content of 28.5-31.5%.

2.2. Mixture proportions

The water-to-cement ratio of 0.35 was selected for the microconcrete mix, based on the recommendations provided by the RILEM - CT 255 SAP [14] technical committee for inter-laboratory tests on high-strength microconcretes. To standardize the experiments and adjust the superplasticizer

content, the spread was set at 190 ± 10 mm. The consistency of the microconcretes was assessed using the Hagermann truncated cone mold in accordance with DIN 18555 - 2 [15], without tapping on the table. The metakaolin content in the mixtures was maintained at 10% of the Portland cement mass. Table 4 shows the composition of the mix utilized for molding high-strength microconcrete specimens for microtomographic analyses. The dry materials were initially mixed, and then water was added, along with the dissolved superplasticizer additive to improve the dispersion of cement grains and other materials.

Table 4. Microconcrete Mix Designs. Microconcrete mixes. C - Cement; MK - Metakaolin; A - Sand; SP - Superplasticizer.

Mix	C (g)	MK (g)	A (g)	Theoretical Water (ml)	Water Absorption by Sand (ml)	Water Content in Superplasticizer (ml)	Total Water (ml)	SP (g/m^3)	SP (%)
MKR	700	70	1340	245	13.40	4.90	253.5	7.0	1.0

The mixes were prepared using a 1200 W power mixer with a frequency of 60 Hz and adjustable rotation ranging from 0 to 650 rpm. The mixer had dimensions of 410 x 290 x 200 mm.

2.3. X – Ray microtomography

2.3.1. Preparation of samples and testing method.

Cylindrical specimens measuring ø2x4cm were molded in a single layer and subsequently placed in a humid chamber, with the vitreous material being used to seal the surface of the samples to prevent drying. High-resolution X-ray micro-CT scans of the samples were carried out using the Zeiss Xradia Versa 510 system, which generates X-rays with cone beam geometry. These tests were conducted at the Digital Materials Laboratory of the Fluminense Federal University (UFF). The image acquisition process involved a rotating base, where the sample was kept stationary in the equipment, as depicted in Figure 2a. The source was held constant, and the object was rotated around an axis, as illustrated in Figure 2b. The set of acquired grayscale 2D images were used for subsequent analyses.

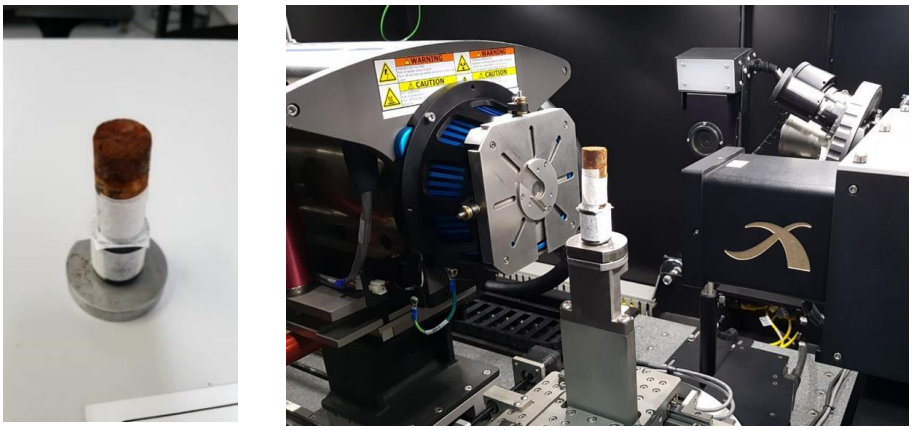

a) b)

Figure 2. Microconcrete testing in the tomograph. a) Test specimen attached to the rotating fixation base. b) Test specimen positioned in the image acquisition equipment.es), it is possible to form a digital three-dimensional object.

In this study, the distances between the source-sample and source-detector were adjusted to obtain a pixel resolution of 20µm. Both the source and detector moved to acquire the images. The distances were balanced to achieve the determined resolutions.

2.3.1. Image Processing and Analysis

The image analysis methodology was based on previous studies by Gomes [16], Enríquez-León et al. [8], and Aboufoul, Garcia [17]. The Fiji/ImageJ software [18] was employed for all image analysis procedures, including the pre-processing of tomographic images. Histogram equalization was initially performed to redistribute the gray scale of the image pixels, which is necessary for an accurate image segmentation in the subsequent stage of the experimental program. This step ensures a more uniform distribution of pixel percentages across the gray scale of the histogram, resulting in a more homogeneous image, as depicted in Figure 3.

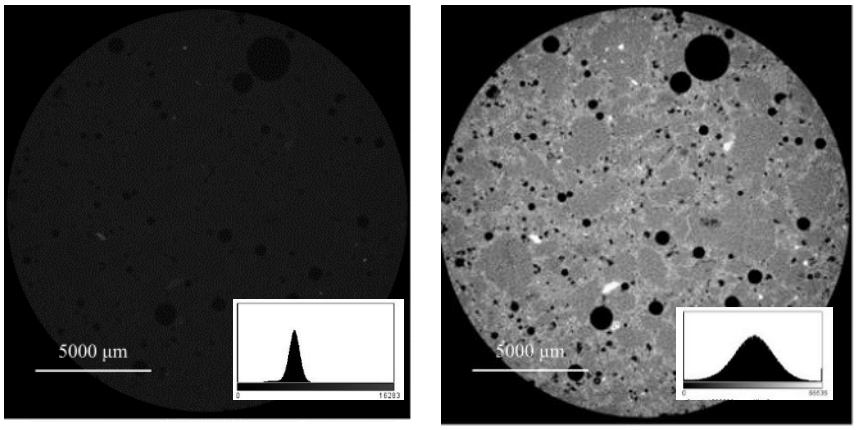

a) b)

Figure 3. Effect of histogram equalization on images. a) Natural image, without treatment; b) Image after histogram equalization.

To improve image quality, a Non-local means denoising filter (NML) with sigma = 10 and smoothing factor = 2 was applied to the micro-CT images. After filtering, image segmentation was performed using the Threshold (TH) tool in Fiji/ImageJ. The TH tool selects a certain threshold value and binarizes the image, segmenting regions of interest. The parameters for the TH segmentation technique were based on previous research by Enríquez-León et al. [8] and Matanna, Pereira, and Costa [19]. To evaluate the effectiveness of the segmentation technique, segmentation was performed 11 times with different threshold values for the image grayscale range.

The conversion of the images from 32 to 8 Bits was carried out to simplify the process of image segmentation. This conversion reduced the grayscale range of the image to 0-255, which facilitated the selection of the appropriate range for each region of interest for the analyzed elements. The grayscale tones of the image are represented on a scale of 0 to 255, where 0 indicates black, 255 indicates white, and the other grayscale tones are distributed between these two values. Promentilla and Sugiyama [20] suggest determining the TH values for segmentation by identifying the peak of grayscale tones in the histogram and dividing this value into two equal parts. Thus, a TH value of 74 was established to define a pore within the 255-grayscale range. The subsequent segmentations were carried out using this TH value, as illustrated in Figure 4.

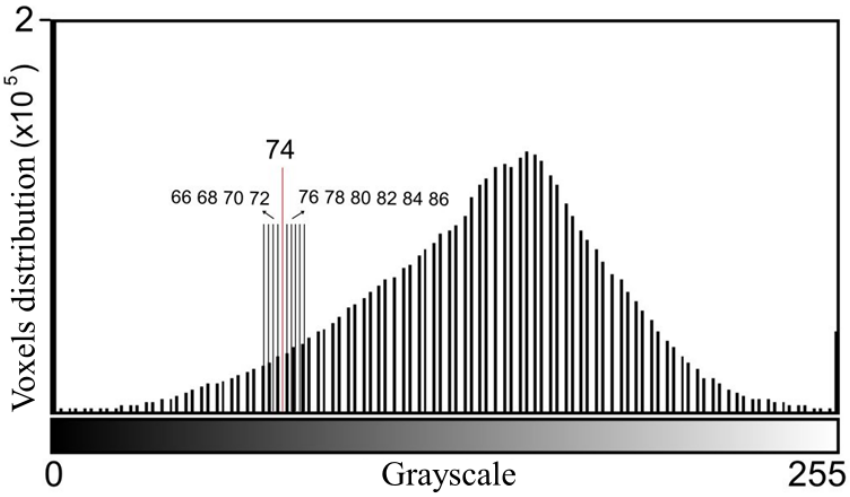

Figure 4. Grayscale ranges of the microtomography and the TH regions segmented from the base TH (74)

A range of 66 to 86 was selected as the limits for the threshold, based on the observation that pores were being excluded or mortar was being included in the segmentation when using lower or higher values, respectively. The segmented images were then processed using the Kill Borders and Morphological Operations (MOP) plugins to eliminate small noise artifacts caused by the segmentation process. The MOP parameters included erosion (r = 1), dilation (r = 1), Geodesic reconstruction (dilation and connectivity = 4), and 3D despeckle. The comparison of porosity values for each threshold was performed to determine if the variation in porosity was significant or not and to evaluate the impact of the threshold on the final results. This comparison was carried out with the purpose of verifying the sensitivity of the method to the chosen threshold

III. DISCUSSION AND RESULTS

After conducting multiple segmentations, a 3D representation of the intrinsic porosity for each segmentation was obtained. This visualization offers an initial understanding of the impact of altering the threshold on the porosity outcomes of the specimens. Figure 5 illustrates the pore structure generated for threshold values of 66, 74, and 86, which correspond to the lower limit, the operator-determined optimal value, and the maximum limit value defining a pore, respectively.

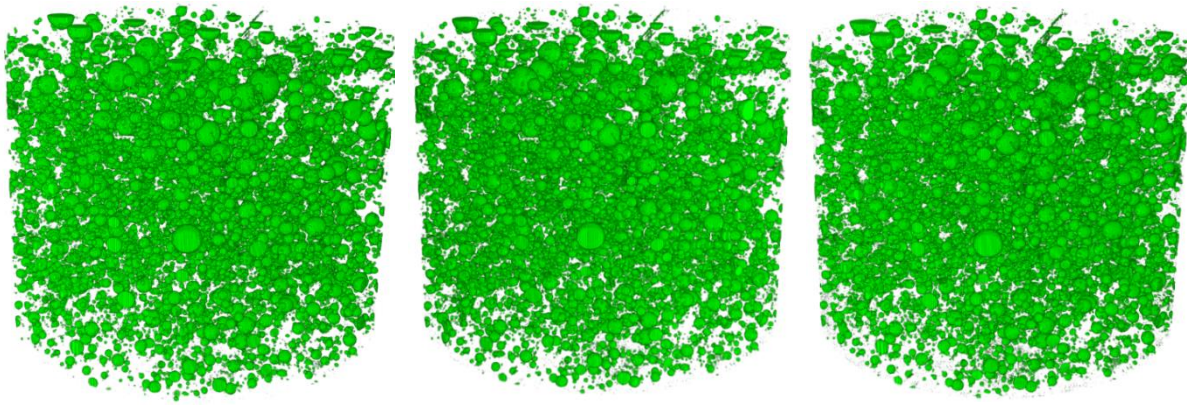

Figure 5. 3D visualizations of the formed porosity for different threshold values during the segmentation step.

After comparing the segmented porosity using different threshold parameters, it can be preliminarily concluded that there are no significant differences between the results. Despite the 20-grayscale value difference between the lowest and highest analyzed threshold, there is minimal alteration in the porosity structure detected. This outcome indicates a reasonable range of thresholds to be used when segmenting a Region of Interest (ROI) in an X-ray microtomography image of concrete or hardened cementitious material. However, visual analysis of 3D renderings and comparison of 2D slices of the specimens' tomography cannot be considered as a conclusive outcome, but rather an initial step towards comprehending the variations in porosity obtained using this technique. Therefore, to carry out a more comprehensive analysis on this topic, the percentage of macro porosity for each determined threshold was calculated, and its results can be observed in Figure 6.

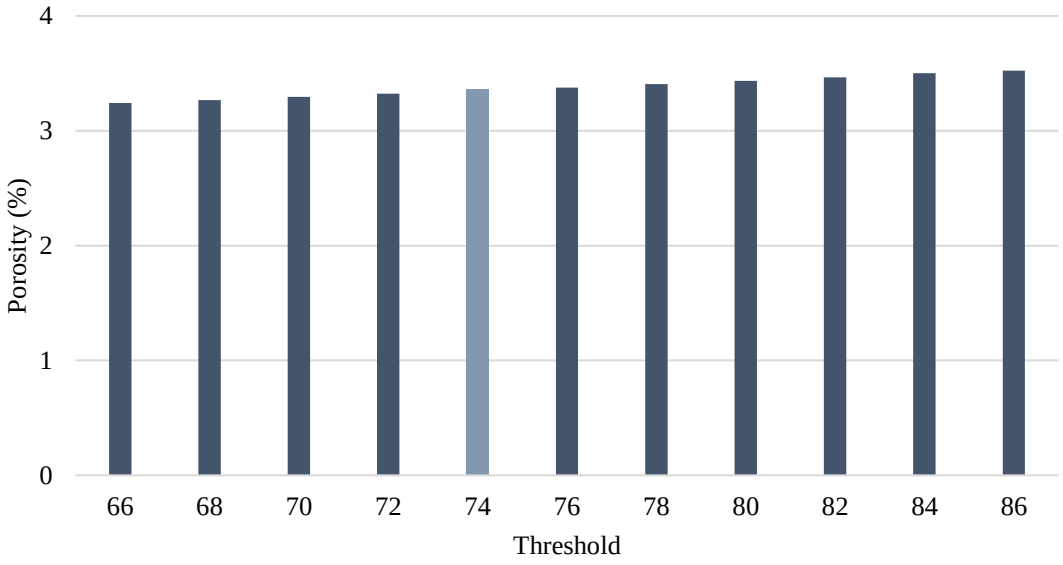

Figure 6. Relative percent porosity for each TH value

Based on Figure 6, it can be deduced that despite the 20-point difference in TH values, the variation in porosity was only 0.29%. Consequently, although the porosity does change with the TH value, values within a range of 10 to 20 points appear to have no substantial influence on the final outcome. It is noteworthy that in this investigation, the minimum and maximum TH values were established to reflect the situation in which the image processing program operator would visually examine the images to determine an appropriate TH. Thus, even if there were variations in TH definition due to human error in the analysis, the variation in percentage porosity would be small, as covered by the minimum and maximum values established in this study. While percentage porosity does not exhibit significant changes with TH variation, the same does not hold for the number of pores found. Figure 7 presents the number of pores identified in the analyses according to the established TH. In summary, the number of pores found increases significantly with TH variation.

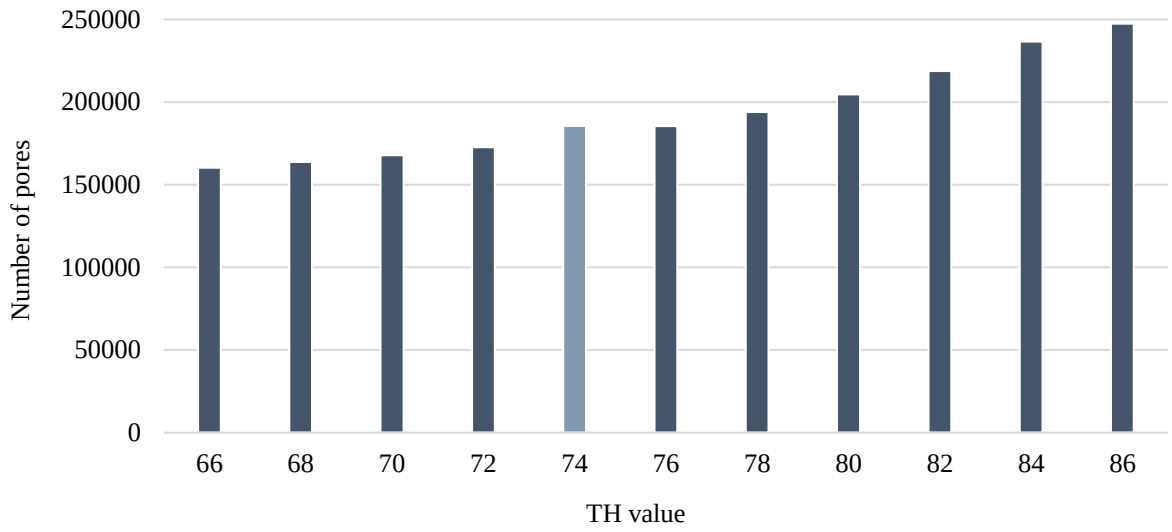

Figure 7. Number of pores found according to the chosen TH.

Based on the analysis, it was observed that for a TH of 66, a total of 160,171 pores were detected, while for a TH of 86, the value increased to 247,453. However, it is important to note that this count is not an exact representation of the total number of pores present in the 3D microtomography, as multiple counts could be made for the same pore in different 2D slices. Despite this limitation, this number still provides an insight into the difference in the quantity of pores detected by the chosen TH. Notably, the increase in TH leads to a significant increase in the number of pores detected, which could have been missed by a lower TH. These pores occupy a small area and are responsible for the increase in porosity by only 0.29%. Nevertheless, the number of pores detected increases substantially as the TH increases, demonstrating the significant impact of the TH parameter on pore detection.

The observed increase in the number of detected pores as the TH increases can be explained by the fact that a higher threshold allows for the detection of smaller pores that were previously missed by the lower threshold. This increase in pore detection is a positive outcome for material characterization and analysis, as it provides more comprehensive information about the pore structure of the material under study. However, it is important to carefully consider the implications of this increased sensitivity to small pores, as they may not necessarily be of significant importance for the material's overall performance.

Furthermore, it is noteworthy that the number of pores detected has a direct influence on the material's permeability, as a higher number of smaller pores would lead to increased permeability. Therefore, understanding the impact of the TH parameter on pore detection is crucial for accurately characterizing a material's porosity and permeability, which are important factors in determining its mechanical and chemical properties.

Finally, the sensitivity of the TH parameter to pore detection emphasizes the need for a consistent and reliable thresholding approach in microtomography image analysis. This can be achieved through the development of automated image analysis techniques that minimize the potential for human error and ensure consistent and accurate results. Overall, the study highlights the importance of carefully selecting and optimizing the TH parameter for accurate and reliable material characterization using X-ray microtomography.

IV. CONCLUSIONS

This investigation has shed light on the behavior of porosity in specimens studied using the X-ray microtomography technique, specifically through the manual segmentation process utilizing the Threshold tool. The results indicate that within the range of TH variation analyzed (66 to 86 points on the grayscale), no significant changes were observed in the determined porosity percentage. Hence, in cases where the analysis is limited to this parameter, any potential human error in the manual

segmentation process can be overlooked, given that it has minimal effect on the final outcome, even when a wide range of variation is present.

However, it is worth noting that concerning the number and area of pores, the variation becomes significant when the TH is altered. Therefore, it is of paramount importance to perform the segmentation process meticulously, especially when analyzing the number or size distribution of pores, such as in the case of porous diameter distribution. Through careful and accurate segmentation, erroneous results regarding the porosity of the analyzed material can be avoided.

ACKNOWLEDGEMENTS

The authors would like to express our sincere gratitude to the following institutions for their invaluable support and contributions to this study: The Digital Materials Laboratory at the Federal Fluminense, the Coordination for the Improvement of Higher Education Personnel (CAPES) of Brazil and the University of Bras

REFERENCES

[1] Pereira, A. (2016). Experiências na engenharia da UFF com micro tomografia de raios-X. História, histórias, 2(11), 18-33.

[2] Landis, E. N., Nagy, E. N., & Keane, D. T. (1997). Microtomographic measurements of internal damage in portland-cement-based composites. Journal of Aerospace Engineering, 10(1), 2-6.

[3] Bernardes, E. E., de Magalhães, A. G., Vasconcelos, W. L., Carrasco, E. V. M., Nunes, E. H. H., & de Lima, L. B. (2017). Characterization of test specimens produced in reduced size for X-ray microtomography (μ-CT) tests. Revista IBRACON de Estruturas e Materiais, 10(5), 1025-1041. http://dx.doi.org/10.1590/s1983-41952017000500005.

[4] Vianna, R. S., Silva, L. C., Lopes, R. T., Ribeiro, L. M., & De Andrade, R. J. (2020). Computing Effective Permeability of Porous Media with FEM and Micro-CT: An Educational Approach. Fluids, 5(1), 16. (4)

[5] Rattanasak, U., & Kendall, K. (2005). Pore structure of cement/pozzolan composites by X-ray microtomography. Cement and Concrete Research, 35, 637-640.

[6] Palma e Silva, A. A., Capuzzo, V. M. S., Silva, E. F., Pereira, A. M. B., & e Silva, D. A. P. (2022). Evaluation of mechanical properties and microstructure of high-performance mortars with superabsorbent polymers and metakaolin by means of X-ray computed microtomography. Journal of Building Engineering, 51, 104219.

[7] Meira, S. A., Sacramento, L. A., Lima, M. P., de Castro Pessôa, J. R., de Almeida Nascimento, F. L., & de Assis, J. T. (2020). Análise da porosidade de concreto por processamento de imagem: uma visão da sensibilidade do Threshold na binarização. Brazilian Journal of Development, 6(3), 16449-16459.

[8] Enríquez-León, A. J., de Souza, T. D., Aragão, F. T. S., Braz, D., Pereira, A. M. B., & Nogueira, L. P. (2021). Determination of the air void content of asphalt concrete mixtures using artificial intelligence techniques to segment micro-CT images. International Journal of Pavement Engineering, 1-10.

[9] ASSOCIAÇÃO BRASILEIRA DE NORMAS TÉCNICAS. (2018). NBR, ABNT 16697: Cimento Portland — Requisitos. Rio de Janeiro.

[10] ASSOCIAÇÃO BRASILEIRA DE NORMAS TÉCNICAS. (2018). NBR, ABNT. 16607: Cimento Portland—Determinação dos tempos de pega. Rio de Janeiro: ABNT.

[11] ASSOCIAÇÃO BRASILEIRA DE NORMAS TÉCNICAS. (2017). NBR, ABNT. 16605: Cimento Portland e outros materiais em pó: determinação da massa específica.

[12] ASSOCIAÇÃO BRASILEIRA DE NORMAS TÉCNICAS. (2019). NBR NM 67:2019 - Concreto - Determinação da resistência à compressão de corpos de prova cilíndricos. Rio de Janeiro: ABNT.

[13] ASSOCIAÇÃO BRASILEIRA DE NORMAS TÉCNICAS. (2010). NBR 7211:2010 - Agregados para concreto - Especificação. Rio de Janeiro: ABNT.

[14] RILEM. (2012). State-of-the-art report of the Rilem Technical Committee 225-SAP: Application of superabsorbent polymers (SAP) in concrete construction. Mechtcherine, V. & Reinhardt, H.W. (Eds.). London: Ed. Springer. (12)

[15] Deutsches Institut für Normung. (1982). 18555-2: Testing of mortars containing mineral binders, freshly mixed mortars containing aggregates of dense structure (heavy aggregates), determination of consistence, bulk density and air content. DIN, Germany.

[16] Gomes, O. F. M. (2001). Processamento e Análise de Imagens Aplicados à Caracterização Automática de Materiais. Dissertação apresentada ao Departamento de Ciência de Materiais e Metalurgia da PUC/Rio como parte dos requisitos para a obtenção do título de Mestre em Ciências da Engenharia Metalúrgica.

[17] Aboufoul, M., & Garcia, A. (2017). Factors affecting hydraulic conductivity of asphalt mixture. Materials and Structures, 50(1), 1-16.

[18] Schindelin, J. (2012). FIJI. An Open-Source Platform for Biological-Image Analysis. Nature Methods, 9, 676-68. (17)

[19] Mattana, A. J., Pereira, E., & Costa, M. M. M. (2014). Evaluation Of Porosity In Mortar By X-Ray Microtomography (Micro-CT). As an additional tool for mercury intrusion porosimetry. Iberoamerican Journal of Applied Computing, 4(1).

[20] Promentilla, M. A. B., & Sugiyama, T. (2010). X-Ray Microtomography of Mortars Exposed to Freezing-Thawing Action. Journal of Advanced Concrete Technology, 8(2), 97-111.

[21] Augusto, K. S., & Paciornik, S. (2017). Porosity characterization of iron ore pellets by X-ray microtomography. Materials Research, 21(2), e2017062.

[22] Legland, D., & Arganda-Carreras, I. (2016). Morpholibj User Manual. Institut National de la Recherche Agronomique: Nantes, France.